

The multipopulation phenomenon in Galactic globular clusters: M4 and M22

S. Villanova,¹ G. Piotto,² A. F. Marino,² A. P. Milone,² A. Bellini,²
L. R. Bedin,³ Y. Momany⁴ and A. Renzini⁴

¹Departamento de Astronomía, Universidad de Concepción, Casilla 160-C, Concepción, Chile
email: svillanova@astro-udec.cl

²Dipartimento di Astronomia, Università di Padova, Vicolo dell'Osservatorio 3, Padova,
I-35122, Italy

email: giampaolo.piotto,anna.marino,antonino.milone,andrea.bellini@unipd.it

³Space Telescope Science Institute, 3700 San Martin Drive, Baltimore, MD 21218, USA
email: bedin@stsci.edu

⁴Osservatorio Astronomico di Padova, Vicolo dell'Osservatorio 5, 35122 Padova, Italy
email: yazan.momany,alvio.renzini@oapd.inaf.it

Abstract. We present an abundance analysis based on high-resolution spectra of red-giant-branch (RGB) stars in the Galactic globular clusters NGC 6121 (M4) and NGC 6656 (M22). Our aim was to study their stellar population in the context of the multipopulation phenomenon recently discovered to affect some globular clusters. Analysis was performed for the following elements: O, Na, Mg, Al, Ca, Fe, Y, and Ba. Spectroscopic data were completed by high-precision wide-field $UBVI_C$ ground-based photometry and *HST*/ACS observations. For M4, we find a well-defined Na–O anticorrelation composed of two distinct groups of stars with significantly different Na and O content. The two groups of Na-rich and Na-poor stars populate two different regions along the RGB. As regards M22, Na and O follow the well-known anticorrelation found in many other GCs. However, at odds with M4, it appears to be continuous without any hint of clumpiness. On the other hand, we identified two clearly separated groups of stars with significantly different abundances of the s-process elements Y, Zr and Ba. The relative numbers of the members of both groups are very similar to the ratio of the stars in the two subgiant branches of M22 recently found by Piotto (2009). The s-element-rich stars are also richer in iron and have higher Ca abundances. This makes M22 the second cluster after ω Centauri where an intrinsic spread in Fe was found. Both spectroscopic and photometric results imply the presence of two stellar populations in M4 and M22, even if both clusters have completely different characteristics.

Keywords. globular clusters: individual (M 4, M 22)

1. Introduction

Globular clusters (GCs) are generally chemically homogeneous in their Fe-peak elements, while they show star-to-star abundance variations in light elements such as C, N, O, Na, Mg, and Al, among others. In some cases, these chemical inhomogeneities result in well-defined anticorrelations. For example, all GCs for which Na and O abundances have been measured show a well-defined Na–O anticorrelation (see Carretta *et al.* 2006, 2008 for an update). The origin of these variations is not yet well understood, since both a primordial and an evolutionary explanation, or a combination of both have been proposed (see Gratton *et al.* 2004 for a recent review).

Interestingly enough, abundance anomalies have been found also among stars on the lower part of the red-giant branch (RGB) or even on the main sequence (MS). For

instance, Cannon *et al.* (1998) found a CN bi-modality in MS and subgiant-branch (SGB) stars in 47 Tuc, and the Na–O anti-correlation was found at the level of the MS turnoff (TO) and SGB in M 13 (Cohen & Meléndez 2005), NGC 6397 and NGC 6752 (Carretta *et al.* 2005; Gratton *et al.* 2001), NGC 6838 (Ramírez & Cohen 2002). On their own, these results suggest a possible primordial origin for the abundance inhomogeneities.

More recent results, made possible by a significant improvement of the photometric precision of *HST* images, indicate the presence of multimodal sequences in the color–magnitude diagrams (CMDs) of some GCs (Bedin *et al.* 2004; Piotto *et al.* 2007; Milone *et al.* 2008), which further confirms that at least in some GCs there is more than one generation of stars formed from material chemically contaminated by previous generations.

Among the clusters with multiple stellar populations, ω Centauri is the most complex and interesting case. This object is the only GC for which variations in iron-peak elements have been identified unambiguously (Freeman & Rodgers 1975; Norris *et al.* 1996; Suntzeff & Kraft 1996). The Fe multimodal distribution is at least in part responsible for the multiple RGB (Lee *et al.* 1999; Pancino *et al.* 2000) of ω Cen. Its MS also splits into three sequences, as shown by Bedin *et al.* (2004). Recently, Villanova *et al.* (2007) showed that the SGB also splits into at least four branches with a large age difference (greater than 1 Gyr) among the different populations.

NGC 2808 is the second cluster in which a MS split into three branches was found (Piotto *et al.* 2007). The MS multimodality was associated with the observed multimodal distribution of the stars along the Na–O anticorrelation, where three groups of stars with different O (and Na) content were found by Carretta *et al.* (2006).

In NGC 1851, Yong & Grundahl (2008) found abundance variations in various elements by studying a sample of eight RGB stars. Sodium and oxygen follow the Na–O anticorrelation, and evidence of the presence of two groups of stars with different s-process element content, as well as two groups of stars with different CN strength were also found, probably related to the two populations of stars photometrically identified by Milone *et al.* (2008) along the SGB.

2. The case of M4

As far as we know, M4 shows no evidence of multiple stellar populations in its CMD, and its mass ($\log M/M_{\odot} = 4.8$; Mandushev *et al.* 1991) is much lower than the mass of the clusters exhibiting photometric peculiarities discussed above. Chemical abundances of M4 RGB stars have already been measured by different groups. A study by Norris (1981) showed a CN bimodality in M4, e.g., stars of very similar magnitudes and colors have a bimodal distribution of CN band strengths. More recently, Smith *et al.* (2005), studying the fluorine abundance in seven RGB stars in M4, found a large variation in F, which is anticorrelated with the Na and Al abundances. In these previous studies, both an evolutionary and a primordial scenario were taken into account to explain the light-element variations and the CN bimodality in M4.

Variations in light-element abundances are common among GCs and are also present in M4. According to our results based on high-resolution high signal-to-noise ratio (S/N) spectra collected with UVES+FLAMES, sodium and oxygen have very large dispersions and show the typical anticorrelation found in many other GCs (Gratton *et al.* 2004), as shown in Figure 1 (left panel). Our most interesting result is that, thanks to the large number of stars in our sample, we can show that the [Na/Fe] distribution is bimodal (Figure 1, right panel). Adopting an arbitrary separation between the two peaks in Figure 1 (right panel) at ~ 0.2 dex, we obtain for the first group of Na-rich stars a mean

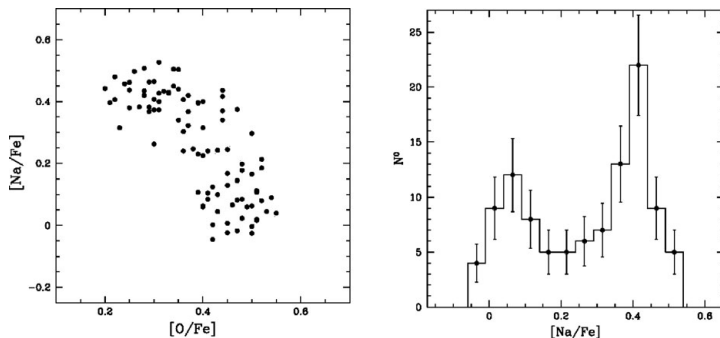


Figure 1. (left) $[\text{Na}/\text{Fe}]$ versus $[\text{O}/\text{Fe}]$ abundance ratios. (right) Histogram of the distribution of the $[\text{Na}/\text{Fe}]$ abundances.

content of $[\text{Na}/\text{Fe}] = 0.38 \pm 0.01$ and $[\text{O}/\text{Fe}] \sim 0.30$ dex, while for the second group of Na-poor stars we get $[\text{Na}/\text{Fe}] = 0.07 \pm 0.01$ and $[\text{O}/\text{Fe}] \sim 0.47$ dex, with a few stars having intermediate sodium and oxygen abundances.

Previous studies also revealed a trend of Na and Al with CN-band strength. The CN-band strengths of red giants in M4 have been measured by many authors, and Smith & Briley (2005) have homogenized all available data for CN-band strengths in terms of the S(3839) index, i.e., the ratio of the flux intensities of the cyanogen band near 3839 Å and the nearby continuum. Figure 2 (left panel) shows the $[\text{Na}/\text{Fe}]$, $[\text{Al}/\text{Fe}]$, $[\text{O}/\text{Fe}]$, $[\text{Mg}/\text{Fe}]$, and $[\text{Ca}/\text{Fe}]$ values we obtained as a function of S(3839) for the stars in common with Smith & Briley (2005). In this figure, CN-strong objects are represented by filled circles, CN-weak by open circles, while open squares are stars in the middle. We note that the CN-strong objects clearly show significantly enhanced Na and depleted O abundances, while the CN-weak stars have lower Na and higher O. There is also a systematic difference in Al between CN-weak and CN-strong stars, with CN-strong stars richer in Al content. Figure 2 shows some differences in $[\text{Mg}/\text{Fe}]$ between the two groups, while no difference is found for Ca.

It is instructive to look at the position of the stars belonging to these two Na groups in the U versus $(U - B)$ CMD (Figure 2, right panel). The Na-rich and Na-poor stars are

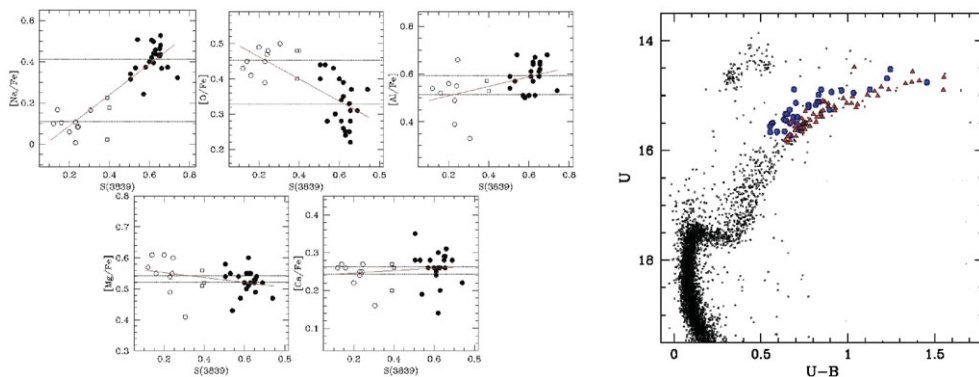


Figure 2. (left) Abundance ratios $[\text{Na}/\text{Fe}]$, $[\text{O}/\text{Fe}]$, $[\text{Al}/\text{Fe}]$, $[\text{Mg}/\text{Fe}]$, and $[\text{Ca}/\text{Fe}]$ are plotted as a function of the CN index S(3839). (right) U versus $(U - B)$ CMD from WFI photometry. The stars belonging to the two different Na groups are represented by two different symbols: red triangles and blue circles represent the stars with $[\text{Na}/\text{Fe}] \geq 0.2$ and $[\text{Na}/\text{Fe}] < 0.2$ dex, respectively.

represented by red triangles and blue circles, respectively. Interestingly, the two groups of Na-rich and Na-poor stars form two distinct branches on the RGB. Na-rich stars define a narrow sequence on the red side of the RGB, while the Na-poor sample populates the blue, more dispersed portion of the RGB. Even more interestingly, the anomalous broadening of the RGB is visible down to the base of the RGB, at $U \sim 17.5$ mag, indicating that the two abundance groups are present all over the RGB, even well below the RGB bump, where no deep mixing is expected. This evidence further strengthens the idea that the bimodal Na, O, and CN distribution must have been present in the material from which the stars we presently observe in M4 originated.

The conclusion is that M4 hosts two groups of stars identified both spectroscopically and photometrically that are due to the presence of two distinct populations. We did not find any dependence of the chemical-abundance distribution on the evolutionary status (along the RGB) of the target stars, from below the RGB bump to the RGB tip. This means that the abundance anomalies are very likely due to primordial variations in the chemical content of the material from which M4 stars formed, and not to different evolutionary paths of the present stellar population of M4. This is surprising because of the relatively low mass of M4, an order of magnitude lower than the masses of ω Cen, NGC 2808, and NGC 1851, the other clusters in which multiple stellar generations have been confirmed. Where did the gas which polluted the material for the CN–Na-rich stars come from? Has it been ejected from a first generation of stars? How could it stay within the shallow gravitational potential of M4? The idea that M4 hosts two generations of stars makes the multipopulation phenomenon in GCs even more puzzling than originally thought. It becomes harder and harder to accept the idea that the phenomenon can be totally internal to the cluster, unless this object is what remains of a much larger system (a larger GC or the nucleus of a dwarf galaxy?). Surely, because its orbit involves frequent passages at high inclination through the Galactic disk, always at distances from the Galactic center of less than 5 kpc (see Dinescu *et al.* 1999), M4 must have been strongly affected by tidal shocks, and therefore it might have been much more massive in the past.

3. The case of M22

Located at a distance of ~ 3.2 kpc (Harris 1996), NGC 6656 (M22) is a particularly interesting GC, because a large number of photometric and spectroscopic studies have suggested a complex metallicity spread, similar to, albeit significantly smaller than, that found in ω Centauri. In particular, it has often been suggested, although never convincingly confirmed, that M22 may also have a spread in the content of its iron-peak elements.

The first evidence for a spread in metallicity comes from the significant spread along the RGB (Hesser *et al.* 1977; Peterson & Cudworth 1994) observed both in $(B - V)$ and in Strömgren colors. However, it is still uncertain whether this spread can be attributed to a metallicity spread or to reddening variations. Spectroscopic studies are divided between those which conclude that no significant metallicity variations are present in M22 (Cohen 1981, based on three stars; Gratton 1982, four stars) and studies claiming a spread in iron, with $-1.4 < [\text{Fe}/\text{H}] < -1.9$ dex (Pilachowsky *et al.* 1984, six stars; Lehnert *et al.* 1991, four stars).

Particularly interesting are the findings regarding the CN-band strengths. Norris & Freeman (1983) showed that CN variations in M22 were correlated with Ca H and K line variations, similar to those in ω Cen. By studying a sample of four stars, Lehnert *et al.* (1991) found Ca and Fe variations that also correlated with variations in CH

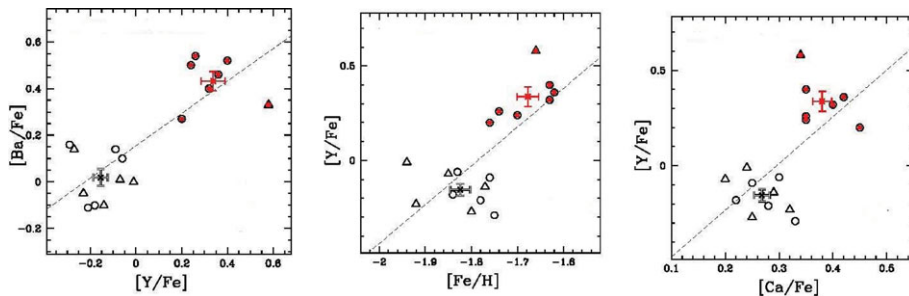


Figure 3. From left to right: $[\text{Ba}/\text{Fe}]$ versus $[\text{Y}/\text{Fe}]$, $[\text{Y}/\text{Fe}]$ versus $[\text{Fe}/\text{H}]$, $[\text{Y}/\text{Fe}]$ versus $[\text{Ca}/\text{Fe}]$ abundance ratios.

and CN-band strength. However, Brown & Wallerstein (1992) found no Ca abundance differences between CN-strong and CN-weak stars, although they observed differences in $[\text{Fe}/\text{H}]$ correlating with the CN strength. More recently, Kayser *et al.* (2008) found some indications of a CN–CH anticorrelation in SGB stars, perhaps diluted by large uncertainties introduced by differential reddening.

For those reasons, we decided to focus our attention on this enigmatic cluster. As for M4, results we obtained are based on high-resolution high-S/N spectra collected with UVES+FLAMES. We found that M22 shows the typical NaO anticorrelation common to all the GCs where Na and O have been measured to date (see Carretta *et al.* 2006). But the most interesting result comes from the heavier elements. We have measured abundance for the three s-process elements yttrium, zirconium, and barium. All span a wide range of abundance values. The maximum variations of $[\text{Y}/\text{Fe}]$, $[\text{Zr}/\text{Fe}]$, and $[\text{Ba}/\text{Fe}]$ have amplitudes of 0.87, 0.73, and 0.65 dex respectively, much greater than the internal error ($\sigma \leq 0.1$ dex).

In Figure 3 (left panel), we show $[\text{Ba}/\text{Fe}]$ as a function of $[\text{Y}/\text{Fe}]$. A clear correlation between the elements is evident. The s-process elements clearly show a bimodal distribution: one group is overabundant in s elements with average values of $[\text{Y}/\text{Fe}] = +0.34 \pm 0.05$, $[\text{Zr}/\text{Fe}] = +0.60 \pm 0.04$, and $[\text{Ba}/\text{Fe}] = +0.43 \pm 0.04$. This group contains seven out of seventeen stars (i.e., $\sim 40\%$ of the full sample studied in this paper). The remaining ten stars have $[\text{Y}/\text{Fe}] = -0.16 \pm 0.03$, $[\text{Zr}/\text{Fe}] = +0.20 \pm 0.03$, and $[\text{Ba}/\text{Fe}] = +0.02 \pm 0.04$. Stars rich in s-process elements are represented by red filled symbols, while s-poor stars are shown as black open symbols. Circles are RGB stars, while triangles are asymptotic giant branch stars. Crosses with error bars indicate the average abundances of the stars in each group.

On the other hand, there is only a partial correlation between Y, Ba, and Zr abundances with Na, O or Al. However, it seems that stars enriched in s-process elements are all Na and Al rich, while the group of stars with lower s-process element abundances spans almost all values of Na and Al abundance.

This scenario is not limited to s-process elements. If we compare the iron abundances with the s-process element abundances, we find a strong correlation, with s-process element-rich stars having systematically higher $[\text{Fe}/\text{H}]$, as shown in Figure 3 (central panel). The two s-process element-rich and poor groups have average $[\text{Fe}/\text{H}]_{\text{s-rich}} = -1.68 \pm 0.02$ and $[\text{Fe}/\text{H}]_{\text{s-poor}} = -1.82 \pm 0.02$ dex, respectively ($\delta[\text{Fe}/\text{H}] = 0.14$ dex). This makes M22 the second cluster after ω Cen showing an intrinsic Fe spread. As shown in Figure 3 (right panel), the Ca abundance is also well correlated with s-process elements. All this seems to suggest that core-collapse supernovae (CCSNe) are the best candidates to produce the iron excess of the second-generation stars. Indeed, would iron

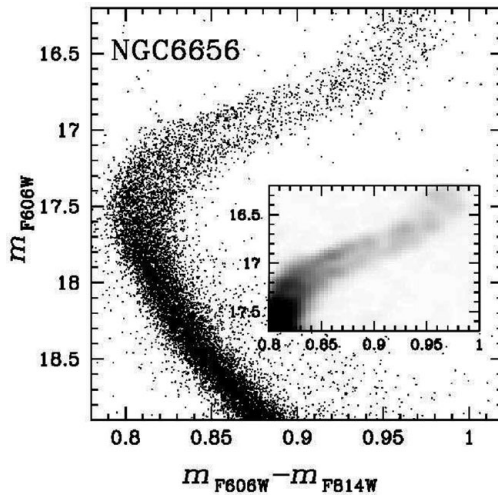


Figure 4. The M22 SGB observed with *HST*.

be produced by Type Ia SNe, we would expect a lower α -element content in s-process-rich stars with respect to the first generation of (s-process element-poor) stars. In fact, SNIa events are selectively enriched in iron. On the other hand, CCSNe along with iron, also produce α elements in higher quantities compared with SNIa.

The bi-modality in s-process elements in M22 resembles the case of NGC 1851. In NGC 1851, Yong & Grundahl (2008) noted that the abundances of the s-process elements Zr and Ba appear to cluster around two distinct values. They suggested that the two corresponding groups of stars may be related to the two stellar populations photometrically observed by Milone *et al.* (2008) along the SGB. At variance with M22, in NGC 1851 the s-element abundance appears to correlate with Na, Al, and O abundance.

From the similarity between our results and those of Yong & Grundahl (2008) for NGC 1851, it is possible to associate the presence of the two groups of stars with different s-process element content with the two populations of stars isolated along the SGB of M22 by Piotto (2009; see also Figure 4). The fraction of stars on the bright SGB corresponds to $62 \pm 5\%$ of the total SGB population, while the faint SGB includes the remaining $38 \pm 5\%$ of the SGB stars. In the stellar sample of the present paper, the fraction of Ba-strong, Y-strong, and Zr-strong stars is $\sim 41\%$. It is therefore tempting to connect the s-process element-poor sample to the bright SGB stars, while the faint SGB stars could have enhanced s-process elements. This second (younger) generation may have formed from material which was also enriched by CCSNe ejecta, as indicated by the higher iron and α -element abundances.

References

- Bedin, L. R., Piotto, G., Anderson, J., Cassisi, S., King, I. R., Momany, Y., & Carraro, G. 2004, *ApJ*, 605, 125
- Brown, J. A. & Wallerstein, G. 1992, *AJ*, 104, 1818
- Cannon, R. D., Croke, B. F. W., Bell, R. A., Hesser, J. E., & Stathakis, R. A. 1998, *MNRAS*, 298, 601
- Carretta, E., Gratton, R. G., Lucatello, S., Bragaglia, A., & Bonifacio, P. 2005, *A&A*, 433, 597
- Carretta, E., *et al.* 2009, *A&A*, 505, 117
- Cohen, J. & Meléndez, J. 2005, *AJ*, 129, 303
- Dinescu, D. I., Girard, T. M., & van Altena, W. F. 1999, *AJ*, 117, 1792

- Gratton, R. G. 1982, *A&A*, 115, 171
- Gratton, R., Sneden, C., & Carretta, E. 2004, *ARA&A*, 42, 385
- Harris, W. E. 1996, *AJ*, 112, 1487
- Lee, Y. W., Joo, J. M., Sohn, Y. J., Rey, S.-C., Lee, H.-C., & Walker, A. R. 1999, *Nature*, 402, 55
- Lehnert, M. D., Bell, R. A., & Cohen, J. G. 1991, *ApJ*, 367, 514
- Milone, A. P., *et al.* 2008, *ApJ*, 673, 241
- Norris, J. 1981, *ApJ*, 248, 177
- Norris, J. & Freeman, K. C. 1983, *ApJ*, 266, 130
- Peterson, R. C. & Cudworth, K. M. 1994, *ApJ*, 420, 612
- Piotto, G., Bedin, L. R., Anderson, J., King, I. R., Cassisi, S., Milone, A. P., Villanova, S., Pietrinferni, A., & Renzini, A. 2007, *ApJ*, 661, 53
- Smith, V. V., Cunha, K., Ivans, I. I., Lattanzio, J. C., Campbell, S., & Hinkle, K. H. 2005, *ApJ*, 633, 392
- Smith, G. H. & Briley, M. M. 2005, *PASP*, 117, 895
- Suntzeff, N. B. & Kraft, R. P. 1996, *AJ*, 111, 1913
- Villanova, S., *et al.* 2007, *ApJ*, 663, 296
- Yong, D. & Grundahl, F. 2008, *ApJ*, 672, 29